Structural Modifications of Surfactant-Assisted Alumina and Their Effectiveness for the Removal of Dyes

Hajira, Tahir*†; Anas, Muhammad.; Uroos, Alam.; Rukhsana, Bibi.Jamil.; Masooda, Qadri
Department of Chemistry, University of Karachi 75270, PAKISTAN

ABSTRACT: *The current study focuses on the development of the modified surface of the alumina by anionic surfactant sodium dodecyl sulfate. The synthesized Surfactant Modified Alumina (SMA) effectively associated with dye molecules and amended their properties. The triphenylmethane (CBB) and thiazine dyes (MB) were selected as a simulated dye wastewater system. The removal was carried out by adsorption method under the optimized amount of adsorbent dosage, the concentration of adsorbate, contact time and temperature. The adsorption isotherm models like Langmuir, Freundlich and Dubinin Radushkevish were employed. The mechanism of the interaction represents the decolorized leuco dye molecules were formed after adsorption. Moreover, the thermodynamic parameters like (ΔS°), (ΔH°) and (ΔG°) were calculated represents the endothermic and spontaneous nature of the adsorption process. The pH at the point of zero charges (pH_{PZC}) was determined. The photocatalytic degradation of respective dye systems was also observed. The surface morphology of (SMA) was determined by FT-IR and SEM techniques. Whereas the pseudo second order kinetics model was followed in the present system. The Pearson correlation Coefficient was conjointly applied. The removal efficiency was ascertained to be 99.50% for CBB(R-250) and 95.70% for (MB).*

KEYWORDS: *Dyes; Adsorption; pH_{pzc}; Kinetics; Thermodynamics; Kinetics.*

INTRODUCTION

The worldwide current scenario where water scarcity is progressively turning into an issue, the pollution of the accessible water resources makes it worse than ever. The removal of pollutants from water has been one amongst the burning issues at this time, particularly dyes containing effluents. Moreover, the textile industrial discharges carry a substantial amount of waste having toxic materials including organic and inorganic contaminants [1]. The characteristic of the toxic stuff is non-biodegradable and has a harmful effect on environment Moreover, it causes varied diseases like contact dermatitis and cancer [2,3].

Textile effluent causes extensive environmental issues and human diseases. The organic materials present in the discharge of dyeing units are of great alarming issue. They react with disinfectants, being volatile in nature and get accumulated into the environment. They are conjointly absorbed through skin and lungs causes irritation and also causes harm to children before birth [4].

** To whom correspondence should be addressed.*
+ E-mail: hajirat@uok.edu.pk
1021-9986/2018/1/47-60 14/$/6.04
DOI:

In order to remove dyes from water there are several techniques including adsorption, electrochemical separation, flocculation, coagulation, membrane filtration etc. are employed but some of them have certain limitations. In the recent era adsorption found to be most successful and convenient method for the removal of colored effluents from the aqueous environment [5]. For this intention, researchers are looking forward to designing economical adsorption model systems, using low cost adsorbing materials including activated carbon, banana pith, orange peel, activated sugarcane bagasse, coir pith, sawdust, natural clays, padded wheat and rice husks [6-13]. The Coomassie Brilliant Blue (CBB, R-250) is a triphenyl methane dye having at least one triphenyl methane group. Moreover, Methylene Blue (MB) belongs to thiazine class dyes that have nitrogen and sulphur containing heterocyclic groups respectively. Whereas CBB (R-250) is an acidic and MB is basic in nature, both of them have industrially wide applications [14-16].

Moreover, the surfactants [17] have an amphiphilic nature, they contain both hydrophilic and oleophilic ends in their structure [18-20]. The molecules of them aggregated over solid surfaces and forms micelles by solubilization process [21]. Since most of the dyes are organic in nature and these micelles structures have a tendency to solubilize the organic molecules. The researchers show their interest towards the application of surfactant-modified solids for the removal of dyes. Several surfactant modified metal oxides have been reported for the removal of dyes and metals [22].

The Al_2O_3 depends on their specific form and applications it could be called alumina, aloxide, or alundum, in general aluminium (III) oxide. Corundum is the most common crystalline mineral of Al_2O_3 exists in polymorphic phase α-Al_2O_3, varieties of which form the precious gems ruby and sapphire.

In the recent study surfactant, modified alumina (SMA) was used for the removal of CBB (R-250) and MB. The applications of SMA for the removal of phenol, Malachite Green (MG) and Crystal Violet (CV) have also been reported [23].

EXPERIMENTAL SECTION

Preparation of Surfactant Modified Alumina (SMA)

The present work represents the preparation of Surfactant Modified Alumina (SMA). For the preparation of SMA, approximately 50 g of alumina was mixed with sodium dodecyl sulphate with a concentration of 250 mg/L. The pH of the solution was maintained at approximately 6.5-7.0, which enhances the adsorption capacity of alumina for SDS. The electrolyte NaCl was also added to the content. The resulting solution was kept in the shaking incubator for 12 hours for shaking at 30 °C. After the specific shaking time interval, the whole content was filtered and washed several times with distilled water and oven dried at 80 °C [24]. The dried SMA was stored in desiccators for adsorption studies.

Preparation of stock solution of dyes

The stock solution of 4.82×10^{-5} M CBB (R-250) and 1.98×10^{-5} M MB was prepared and scanned by UV/Visible Spectrophotometer to determine the λ_{max} of respective dyes.

Batch adsorption studies

Optimization of the amount of adsorbent

The optimum amount of adsorbent (SMA) was evaluated at which highest removal efficacy of respective dyes was observed. The experiments were proceeded by 50mL aliquot of each dye. It was introduced in several flasks with different amount of SMA ranging from 0.1g to 1.8g. All the respective flasks were placed in a shaking incubator (JISICO Shaking Incubator) for 30 min shaking period at 303 K for 200rpm. After the specified time interval, the content was filtered and absorbance was recorded by UV/Visible spectrophotometer at λ_{max} of respective dyes.

Optimization of shaking time

Optimum shaking time interval and its effect on the removal of CBB (R-250) and (MB) dyes were studied. The time interval ranged from 5min to 60 min with the optimized amount of SMA.

Optimization of the concentration of dyes

In order to determine the optimized concentration of dyes, assorted dilutions of the stock solutions of dyes were prepared. The concentrations were maintained by following Beer's and Lamberts Law. For CBB(R-250) it was varied from 3.03×10^{-5}-9.08×10^{-5}M and for MB were ranges 1.38×10^{-5}-2.97×10^{-5}M with an optimized amount of SMA and optimized time period [25].

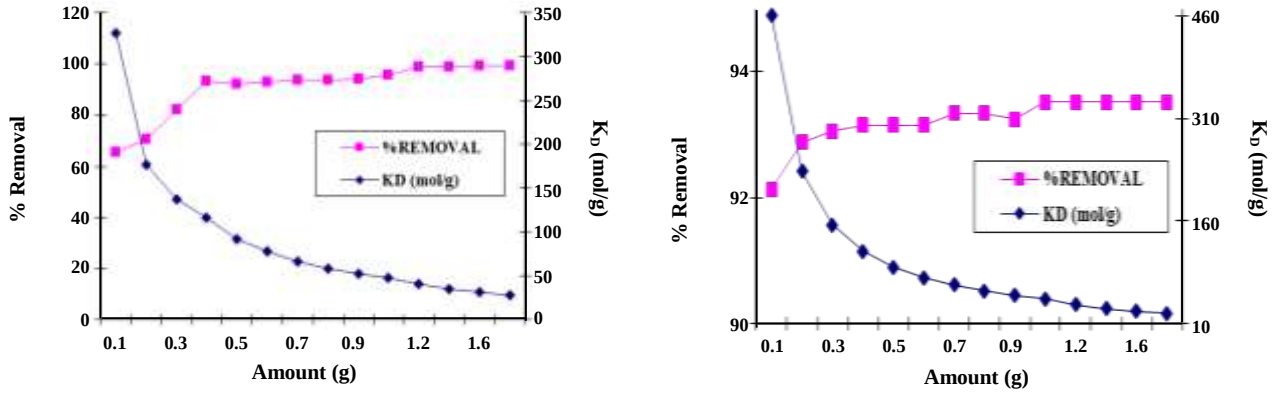

Fig. 2: (a) Effect of adsorbent dosage for the removal of CBB (R-250) by using SMA, (b) Effect of adsorbent dosage for removal of methylene blue by using SMA.

Effect of temperature on adsorption

Adsorption at diverse temperatures was preceded at the optimum amount of SMA and optimized shaking time interval. The flasks were placed in a shaking incubator at 200rpm by varying temperatures 298K - 313K (± 2K) at the step of 5K temperature. The data were incorporated in adsorption isotherm models like Langmuir, Freundlich, and Dubinin-Radushkevich [26]. The values of respective constants were determined graphically.

pH at the point of zero charge PH$_{(PZC)}$

The pH at the point of zero charges (pH_{PZC}) of surfactant-modified alumina (SMA) was determined by pH drift method. The experiment was preceded by taking approximately 50.0mL of 0.005M NaCl solution with an optimized amount of adsorbent. The pH of the respective systems was maintained between 1-14 and monitored at the intervals of 24 and 48 hours [27].

Statistical data analysis

The Pearson Correlation Coefficient analysis was applied to the adsorption data at variables temperatures by using STATISTICA Version 17.

RESULT AND DISCUSSION

Adsorption of CBB (R-250) and (MB) dyes were carried out by SMA functioning as an adsorbent. The adsorption experiments were preceded under the optimized conditions of adsorption. Moreover, the absorbance was measured to determine the removal efficiency of dyes by UV/Visible spectrophotometer. The surface of SMA and its chemical composition was determined by FTIR and SEM techniques.

Investigation of the effects of adsorption parameter

Effect of adsorbent dosage

Adsorbent dosage and its effect on adsorption are of great concern for the removal of dyes. It was observed that the adsorption of dye was enhanced with the increase in active sites of adsorbent. Moreover, adsorption data indicated that %removal of CBB (R-250) and MB dyes were found to be 99.43% and 93.50% at 1.5g and 0.4g of SMA adsorbent dosages respectively. The variation of removal efficiency with the adsorbent dosage is shown in Fig. 2 (a) and (b).

The distribution coefficient K_D (mol/g) and % removal of dyes were calculated as:

$$K_D = (C_i - C_f) \times V/W \quad (1)$$

$$\%\,Removal = (C_i - C_e)/C_i \times 100 \quad (2)$$

Where C_f (M) is the concentration of dye after removal, C_i (M) is the initial concentration of dye in the solution; V is the volume of the solution (mL) and W is the mass of the adsorbent (g). The adsorptive capacity, X/m (mol/g), was calculated as:

$$X/m = (C_i - C_e) \times V/W \quad (3)$$

Where C_e(M) is the equilibrium concentration.

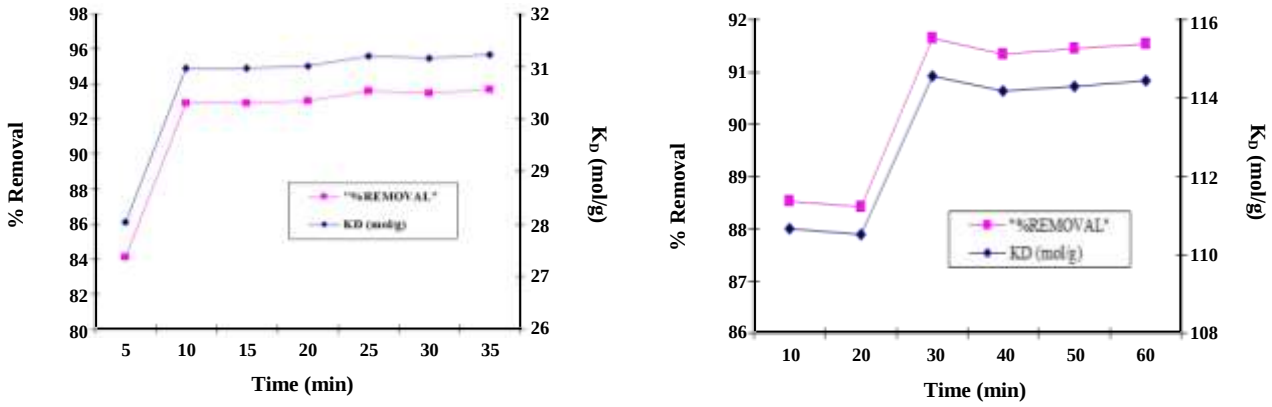

Fig. 3: (a) Effect of contact time for the removal of CBB R-250) by using SMA, (b) Effect of contact time for the removal of methylene blue by using SMA.

Effect of contact time

The removal of CBB (R-250) and MB dyes on SMA was preceded at varying contact time to illustrate the equilibrium time. Fig. 3(a) and (b) show that the rapid increase in % removal was observed at 10 and 30 min in the case of CBB (R-250) and MB dyes respectively. It shows the mechanism that due to the accessible pores on the surface of SMA. The steady occupancy of dye molecules on the surface of SMA makes the removal efficiency less efficient and constant behavior. After that, at equilibrium, the removal efficiency observed to be constant.

Adsorption Isotherms

Adsorption isotherms explain the behavior of the adsorption process. It describes the surface properties and the feasibility of the adsorption process [28,29]. The experimental data were incorporated in Langmuir, Freundlich, and D-R isotherm models.

Langmuir Isotherm model

The Langmuir model assumes that adsorption occurs with monolayer formation onto the uniform surface of adsorbent having a finite number of active sites. The monolayer adsorption could be simply described by Langmuir adsorption isotherm [30]. Moreover, it is represented as:

$$C_e \Big/ \frac{X}{m} = 1/KV_m + C_e/V_m \qquad (4)$$

Where, K is the Langmuir constant and V_m is the monolayer capacity, X/m is the surface coverage to form monolayer and C_e is the equilibrium concentration [31]. The linear plots of Ce /X/m versus C_e were obtained for both dyes system represents the high degree of correlation coefficient as shown in Fig. 4(a) and (b). The Langmuir Constants K and V_m are calculated by gradient and intercept of the respective plots.

Freundlich isotherm

It was analyzed by using following expression:

$$\mathrm{Log}\, X/m = \log K + 1/n \log C_e \qquad (5)$$

Where, *n* and *K* are Freundlich constants that explains the degree of adsorption and it was estimated the intensity of the adsorption respectively [32]. The values of constants K and n are shown in Table 1. The low values of R^2 suggested that the more feasible model is Langmuir isotherm model compared to Freundlich model in the respective system.

Dubinin-Radushkevich (D-R) model

It was analyzed by using following equation:

$$\ln X/m = \ln X_m - K\epsilon^2 \qquad (6)$$

$$\epsilon = RT \ln\left(1 + 1/C_e\right) \qquad (7)$$

Where, X_m is the monolayer capacity, *K* is a constant based on adsorption energy, ϵ is adsorption potential, R is a gas constant, T is absolute temperature, *X/m* and *Ce* have usual meanings. Constants K and X_m were obtained graphically and the mean free energy of sorption (ε_s) were calculated as [33].

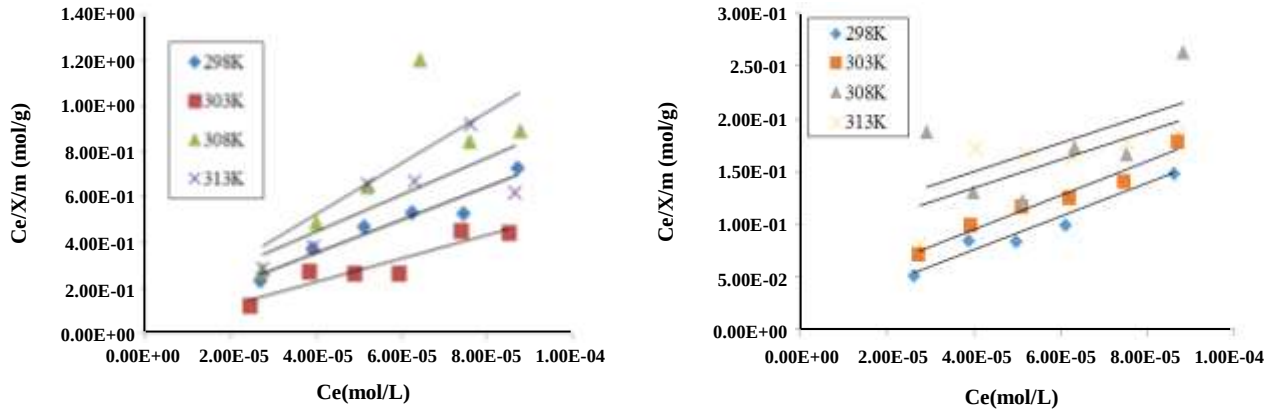

Fig. 4: (a) Langmuir isotherm plots of SMA-CBB (R-250) system, (b) Langmuir isotherm plots of the SMA-MB system.

$$\varepsilon_s = \left(-2K\right)^{-1/2} \tag{8}$$

The low values of R^2 show that the Langmuir model is more favorable compared to the D-R Model. Moreover the adsorption of MB and CBB(R-250) dyes was monitored at temperatures extended from 298 to 313 K and the respective constants from isotherm models are represented in Table 1.

The feasibility characteristics of Langmuir isotherm was determined by a dimensionless constant (R_L), which is represented as:

$$R_L = 1/\left(1+KC_i\right) \tag{9}$$

Where K is the Langmuir constant and C_i the initial concentration. Table 2 shows the R_L values for both dyes systems. The results show that R_L values lie between 0 and 1 indicating the favorable adsorption process.

Effect of thermodynamic parameters

The thermodynamic entities like Gibbs free energy ΔG^0 entropy ΔS^0 and enthalpy ΔH^0 were calculated as:

$$\Delta G^0 = \Delta H^0 - T\Delta S^0 \tag{10}$$

$$Ln\left(K_D\right) = \Delta S^0/R - \Delta H^0/RT \tag{11}$$

$$\Delta G^0 = -RT\ln K_D \tag{12}$$

The K_D represent equilibrium constant obtains from Van't Hoff equation. The R and T are gas constant and absolute temperature respectively [34]. The plot between Van't Hoff ln K_D versus 1/T was used to compute the values of ΔH° and ΔS°.

The negative ΔG^0 values represent the spontaneous nature of the adsorption process at different temperatures. The ΔH° values for CBB (R-250) and MB dyes reveals the endothermic nature of the adsorption process. Whereas the ΔS° values confirm that during the adsorption process at solid–solution interface the increase in randomness was observed [35]. The values of the thermodynamic parameters are shown in Table 3.

Kinetics of adsorption

Adsorption kinetics explains the mechanism of adsorption process and provides useful information regarding factors affecting and controlling the rate of adsorption. It also estimated the effectiveness of the adsorption process [36]. The experimental data was applied in zero order, pseudo-first and second order kinetics models to depict the best fitted kinetic model.

The Lagergren's pseudo-first and pseudo second order [37] expression is represented as:

$$\log\left(q_e - q_t\right) = \log q_e - k_{p1}/2.303t \tag{13}$$

$$t/q_t = 1/k_{p2}q_e^2 + t/q_e \tag{14}$$

Where q_t and q_e (mg/g) are the adsorption capacities. k_1 (min^{-1}) and k_2 (g/g·min) are the pseudo-first and pseudo-second-order rate constants for the kinetic model respectively.

The Plots of t/q_t against t were found to be linear with correlation coefficient 0.999 which correspond that the sorption process follows pseudo-second-order kinetics as shown in Fig. 5 (a) and (b).

Table 1: Parameters of adsorption isotherm models.

Dyes	Temp (K)	.Langmuir Parameters			Freundlich Parameters			D-R Parameters		
		K_L (10^{-4})	V_m (10^4)	R^2	K_F (10^4)	n	R^2	X_m (10^4)	ε_s (10^{-4})	R^2
Coomassie Brilliant Blue CBB (R-250)	298	10.77	1.39	0.933	4.07	7.93	0.299	2.15	2.236	0.291
	303	25.90	1.93	0.864	2.41	5.71	0.066	2.06	5.000	0.005
	308	142.0	0.09	0.599	0.00	3.15	0.021	0.55	2.886	0.024
	313	6.28	1.24	0.631	3.25	8.19	0.069	1.73	2.357	0.064
Methylene Blue	298	14.50	6.0	0.942	23.0	6.94	0.315	11.0	2.236	0.316
	303	5.38	6.0	0.963	72.0	3.55	0.844	0.0	1.581	0.845
	308	1.42	7.0	0.350	342.8	1.41	0.581	108.0	0.912	0.596
	313	1.68	7.0	0.588	153.0	2.61	0.448	22.0	1.290	0.434

Table 2: Langmuir RL constant for the adsorption of CBB (R-250) and MB Dyes on SMA at variable temperatures.

Dyes	Conc. (M) (10^5)	Langmuir constant (R_L)			
		298 K	303 K	308 K	313 K
Coomassie Brilliant Blue CBB (R-250)	3.03	0.2344	0.1131	0.0226	0.3443
	4.24	0.1795	0.0835	0.0162	0.2729
	5.45	0.1455	0.0662	0.0127	0.2260
	6.60	0.1232	0.0553	0.0105	0.1943
	7.87	0.1054	0.0468	0.0088	0.1682
	9.06	0.0927	0.0408	0.0076	0.1491
Methylene Blue	1.38	0.3332	0.5736	0.8353	0.8109
	1.58	0.3038	0.5402	0.8158	0.7893
	1.78	0.2792	0.5105	0.7972	0.7688
	2.17	0.2411	0.4610	0.7633	0.7318
	2.57	0.2115	0.4193	0.7314	0.6973
	2.97	0.1884	0.3846	0.7021	0.6659

Table 3: Thermodynamic parameters for the adsorption of CBB (R-250) and MB Dyes on SMA.

Dyes	Conc.(M) (10^5)	ΔH^o (KJ/mol)	ΔS^o (KJ/mol)	ΔG^o (KJ/mol)			
				298 K	303 K	308 K	313 K
Coomassie Brilliant Blue CBB(R-250)	3.03	2.911	0.037	-8.294	-8.482	-8.670	-8.858
	4.24	0.773	0.031	-8.465	-8.620	-8.775	-8.930
	5.45	1.725	0.034	-8.496	-8.668	-8.839	-9.011
	6.60	1.769	0.034	-8.512	-8.685	-8.857	-9.030
	7.87	1.514	0.033	-8.529	-8.697	-8.866	-9.030
	9.06	0.176	0.029	-8.555	-8.701	-8.848	-8.994
Methylene Blue	1.38	3.324	0.050	-11.64	-11.89	-12.14	-12.39
	1.58	2.362	0.047	-11.73	-11.97	-12.20	-12.44
	1.78	2.108	0.046	-11.74	-11.97	-12.21	-12.44
	2.17	1.666	0.045	-11.77	-12.00	-12.22	-12.45
	2.57	0.655	0.041	-11.82	-12.03	-12.24	-12.45
	2.97	0.733	0..042	-11.79	-12.00	-12.21	-12.42

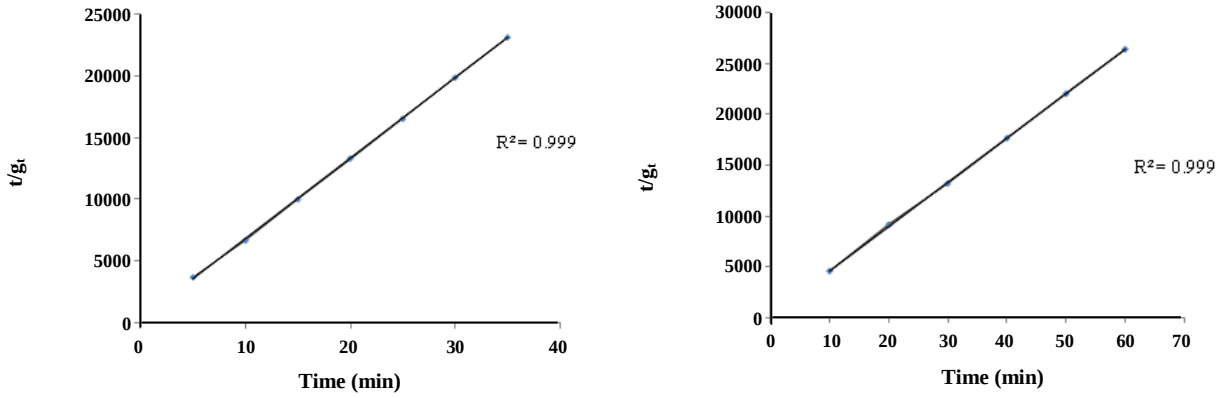

Fig. 5: (a) Plot of pseudo-second-order kinetics for CBB (R-250) and SMA system, (b) Plot of pseudo-second-order kinetics for MB and SMA system.

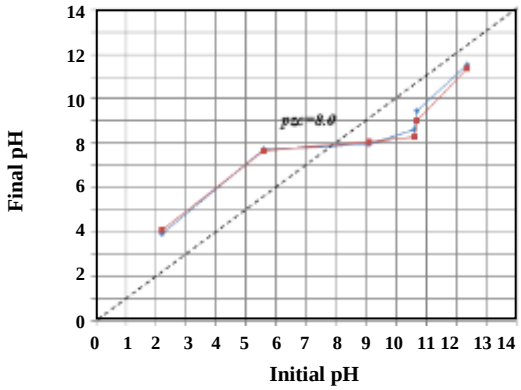

Fig. 6: Effect of PH at pH_{pzc} on the Surface of SMA

Influence of pH at Point Zero Charge (pH_{PZC})

To study the effect of pH at point zero charges (pH_{pzc}), pH drift method was applied. For the investigation of $pH_{(pzc)}$ on the surface of SMA, the values of the pH were examined after 24 and 48hour time interval. The plot of pHs is shown in Fig. 6. The point where $pH_{initial}$ was considered to pH_{final} it corresponds to be pzc ≈ 8 [40]. The results shown in Table 4, represent that the surface of SMA is basic in nature [38].

Mechanism of reversible adsorption

The mechanism of interaction of SMA with MB dye shows that Al_2O_3 acting as adsorbent as interact by Sodium dodecyl sulphate (i.e. anionic surfactant). Initially a monolayer of SDS is formed in such a way that the polar head-group of SDS interact with the oxide surface and its hydrocarbon tail project into solution, forming a hemi micelle. After that, a bilayer of SDS formed due to the hydrophobic interactions between tail-groups, as a result, discrete surface aggregates were formed which are termed as ad micelles. Moreover, the formation of ad micelles are due to the opposite charge interactions which occur between surfactant and alumina [41]. The anionic surfactant is effectively adsorbed on the positively charged alumina surface to form aggregates termed as (hemimicelles). Furthermore, the formation of hemi- and ad- micelles may depend on the concentration of SDS. Additionally, the adminelles interact with MB and CBB dyes and leuco dye is formed which is less toxic.

Moreover, the aluminium trioxide adsorbs the surfactant SDS in presence of water molecule. It resulted in incorporation between the adsorbent and surfactant and produces a field of interaction. Owing to this there was a shifting of electrons and polarity develops in the water layer and the positive charge atmosphere created around the hydrogen atom of the water molecule. Moreover, they attack and lose the electrons from the nitrogen atom of MB and reduced form of leuco dye form. The Fig.7 (a and b) represent a mechanism of dye removal.

The mechanism for the removal of CCB(R-250) by SMA represented that the Al_2O_3 interacts with surfactants SDS and consequently form SMA complex. It has free available electrons on the hydroxyl group and these electrons are interacted by one of the positively charged carbon atoms on the phenyl ring due to the resonating electrons on the ring. Consequently, it causes the degradation via cleavage of conjugated structure and N- methylation also occurred. Moreover, the intermediate products identified as hydroxyl methylation of conjugated triphenyl methane ring [39].

Table 4: Effect of pH at pH(pzc) on the surface of SMA.

Solution pH	Amount of SMA (gm)	Initial pH	pH After 24 Hour	pH After 48 Hour
1.92	1.5	2.19	3.91	4.10
2.83	1.5	5.59	7.73	7.65
6.03	1.5	9.07	7.97	8.07
10.41	1.5	10.60	8.60	8.27
11.18	1.5	10.66	9.45	9.02
12.01	1.5	12.34	11.55	11.36

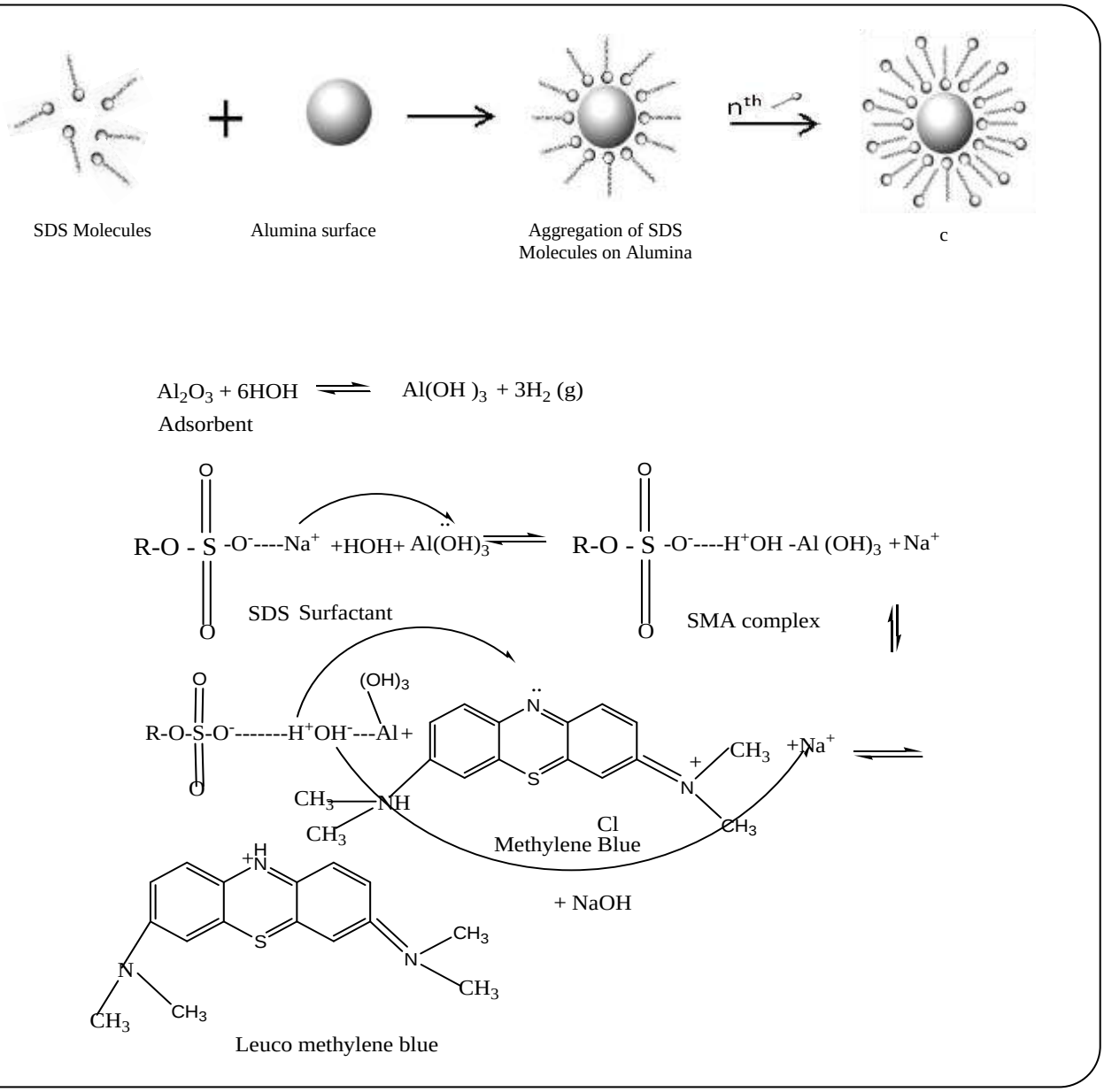

Fig 7(a) Mechanism of formation of surfactant-modified Alumina, (b) Mechanism of reversible adsorption of the SMA and decolorization of the dye (methylene blue).

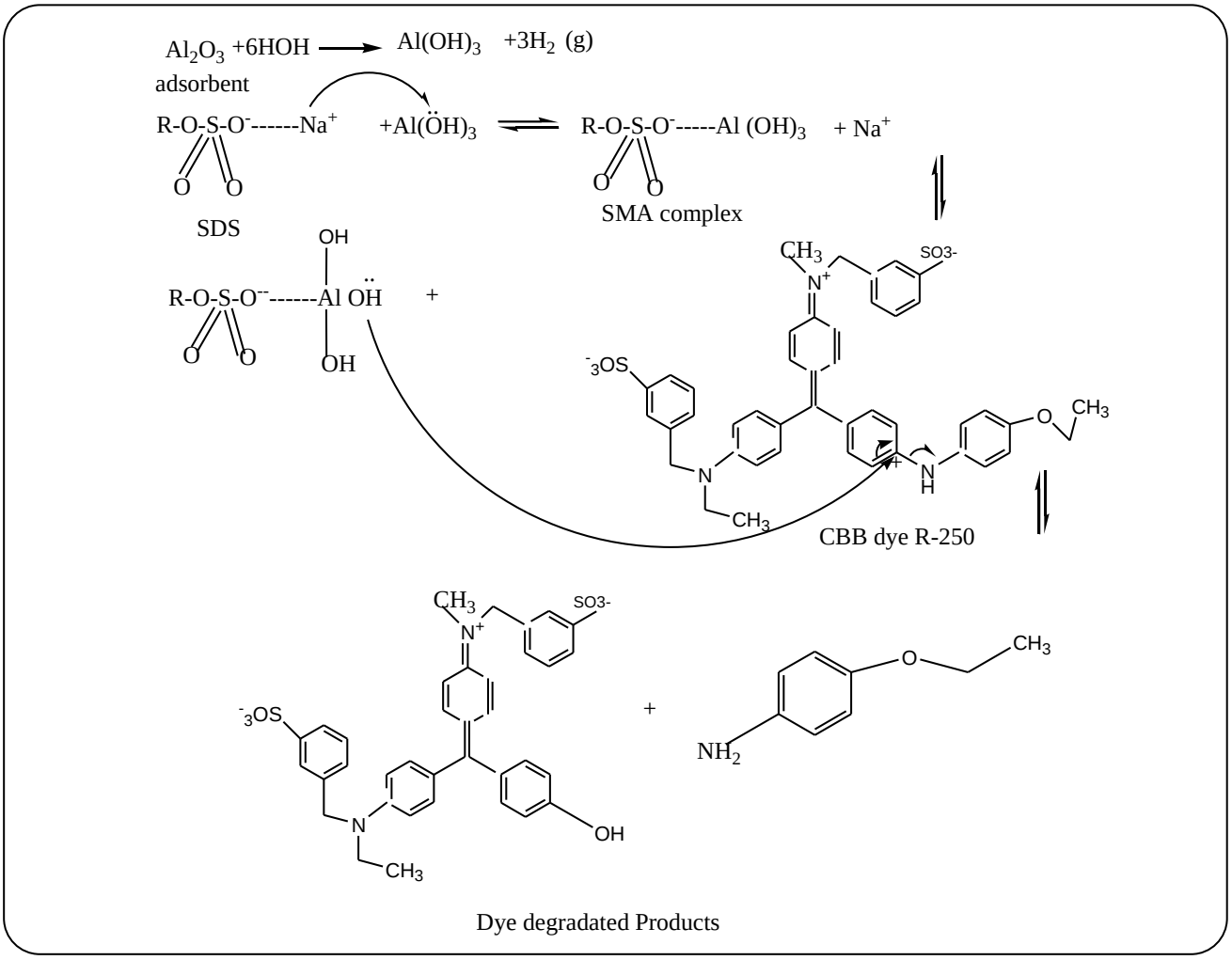

Fig. 7: (c) Mechanism of reversible adsorption of the SMA and decolorization of the dye (Coomassie brilliant blue R-250).

Surface morphology of SMA

FT-IR Spectrum

The Figs. 8 (a-c) represent the FT-IR spectrum of Surfactant Modified Alumina (SMA) samples before and after adsorption with CBB (R-250) and MB respectively. The spectra were recorded in transmittance mode. The reported FTIR spectra of pure Al_2O_3 shows the following characteristic peaks and broad bands, two of the bands appeared at the lower frequency region of 500 - 900 cm^{-1} which were assigned to the Al-O bending vibration and Al-OH wagging [42]. Moreover, some reported data shows that the bands appeared in the region of 500 - 700 cm^{-1} and 700-900 $cm^{-1}$are due to the vibration frequencies of AlO_4 tetrahedron and AlO_6 octahedron network. There was also a broadband observed in the region of 2900 – 3600 cm^{-1} which were due to-OH stretching vibrations [40].

The reported FT-IR spectrum of SDS contains C-H stretching region at (i.e. 2850–2950 cm^{-1}) represent asymmetric and symmetric stretching vibrations of -CH_2- and -CH_3- groups. The CH_2 scissoring region was observed above 1450 cm^{-1}. The CH_2 wagging region observed around 1350 cm^{-1}. Moreover, SO_2 vibration region was observed at (1200 – 1250 cm^{-1}) representing asymmetric and symmetric stretching vibrations of SO_2 group of SDS molecules.

The FT-IR spectral analysis of SMA reveals that there were two sharp peaks observed in the region of 2850-2920 cm^{-1} which indicates the stretching vibrations of -CH_2- group. The small peak appeared around 1470 cm^{-1} was assigned to the deformation of -CH_2- due to the scissoring of -CH_2- group. There were three sharp peaks observed in the region of 1100-1250 cm^{-1} as a doublet

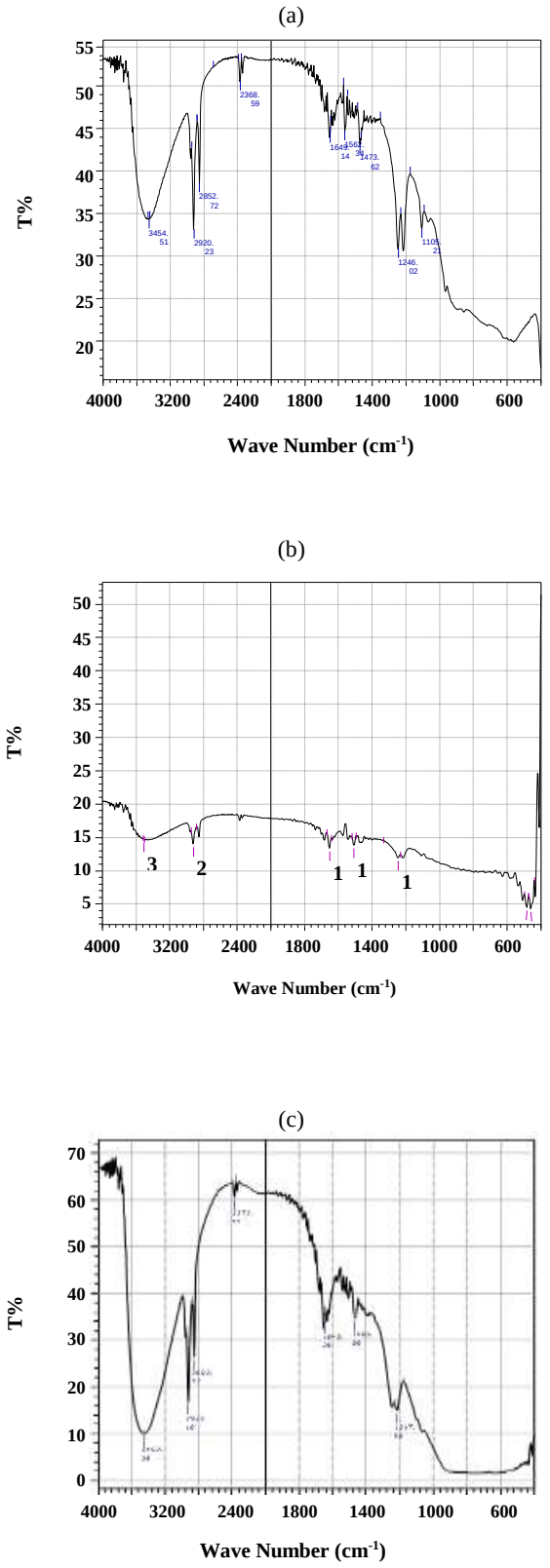

Fig. 8: (a), (b) and (c) represents FT-IR images of SMA, SMA-CBB (R-250) and SMA-MB dyes systems.

which indicates the presence of SO_2 head group of SDS Moreover, they were assigned to the conformational changes and symmetric and asymmetric vibrations of Sulfate respectively. Furthermore, all of the respective peaks are the characteristic peaks of SDS. There was a broadband appeared in the region of 3200-3500 cm^{-1} which shows the existence of -OH group, it usually attached over alumina surface. The peaks in the region of 1550- 1650 cm^{-1} show the presence of some physisorbed water molecules as shown in Fig. 8(a). The peaks were found to be in close agreement with that of the reported data [41].

Moreover, when SMA loaded with CBB (R-250), the whole spectra became intense and there was no significant change in peaks was observed. Furthermore, the peak appeared at 1105.21 cm^{-1} was not found and two other small peaks appeared at the region of 450-500 cm^{-1} which indicates the strong interaction between dye and SMA with the S-O group as shown in Fig. 8(b). A similar trend was observed in case of SMA loaded with MB dye, there were no spectral changes were observed relative to that of Fig. 8(a), but the peaks of SO_2 groups were shifted towards the lower frequency region i.e. 1217.08 cm^{-1}. Moreover, the peak around1105.21 cm^{-1} was disappeared as shown in Fig. 8(c) indicates the interaction of dye and SMA via S-O group.

SEM Scanning

Figs. 9(a), (b) and (c) represents the SEM images of surfactant-modified alumina before adsorption and after the adsorption of CBB (R-250) and MB dyes respectively. The surface of SMA was amorphous in nature with the irregular and non-uniform surface. After adsorption of with dyes, the layer of dye appeared over SMA and the surface became saturated.

Comparative Removal Efficiency

The comparative removal efficiency is represented in Fig. 10. It was observed that Al_2O_3 show about 50% removal efficiency. Moreover, SMA–CBB system dye show 99.5 % removal efficiency. Furthermore, 95.7% removal efficiency was observed by SMA-MB system.

Pearson correlation analysis

The Pearson correlation Coefficient represent that for CBB (R-250) strong correlation was found to be at 313K

Table 5: Pearson correlations coefficients at variable temperatures for the removal of dye by SMA.

Methylene Blue				
Temperatures (K)	303K	308K	313K	318K
303	1			
308	0.971	1		
313	0.222	0.252	1	
318	0.897	0.881	-0.169	1
	Coomassie Brilliant Blue R-250			
Temperatures (K)	303K	308K	313K	318K
303	1			
308	0.939	1		
313	0.964	0.885	1	
318	0.909	0.857	0.930	1

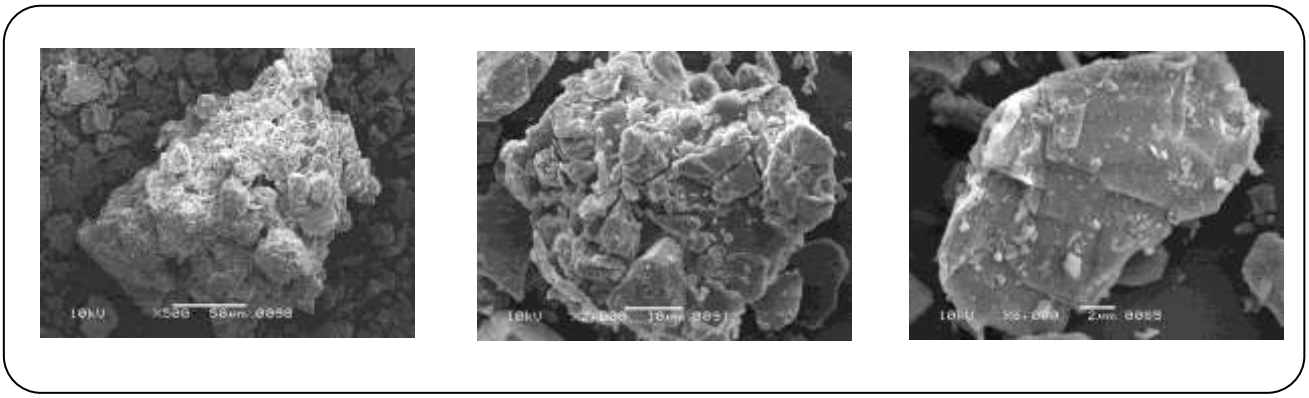

Fig. 9: (a), (b) and (c) represents SEM images of SMA, SMA-CBB (R-250) and SMA-MB dyes.

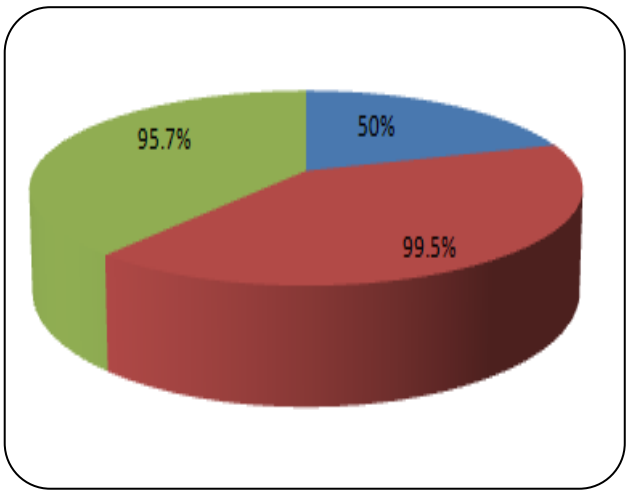

Fig 10: Comparative removal efficiencies of Al_2O_3, SMA-CBB, SMA-MB systems.

about 0.964. For MB system it was observed to be 0.971 at 308K temperature. The values are shown in Table 5.

CONCLUSIONS

In the present study the removal of Triphenylmethane (Coomassie Brilliant Blue (R-250) and thiazine dyes (Methylene Blue) were carried out. Alumina was modified by Sodium dodecyl sulfate and used for the adsorption. Moreover about 99.50% removal was obtained for CBB (R-250) dye and 95.70% for MB dye.

The adsorption studies were applied for the removal of dyes. Moreover, the adsorption isotherm models were employed to determine the feasibility of the process. Furthermore, it was concluded that for CBB (R-250) dye, adsorption was more favorable at high temperatures

although in the case of MB it is dominating at low temperatures. The R_L factor was also calculated which shows that adsorption favors the Langmuir isotherm.

The thermodynamic study was also employed to observe the feasibility of the adsorption process. Moreover, both dye systems show endothermic and spontaneous behaviors.

Adsorption Kinetics was also investigated, both the triphenylmethane and thiazine dyes were found to follow Pseudo-Second order kinetics with a correlation coefficient of about 0.999.

The mechanism of SMA-MB and SMA- CCB(R-250) was also shown representing the decolorized leuco dye formation. The Pearson Correlation Coefficient for both the dye systems was also determined. The low-cost adsorbent can effectively use for the treatment of wastewater.

Acknowledgments

The author acknowledges Department of Chemistry University of Karachi for providing necessary research facilities.

Conflict of Interest: Author has no conflict of interest regarding the submitted manuscript.

Received: May 12, 2016; Accepted: Jul. 10, 2017

REFERENCES

[1] Xu L., Chen C., Na Li., Sun X., Shen J., Li J.S., Wang L., Role of Surfactants on the Hydrolysis and Acidogenesis of Waste-Activated Sludge, *Desalination and Water Treatment*, **57**(35):16336-16345 (2016)**.**

[2] Specht K., Platzek, Textile Dyes and Finishes-Remarks to Toxicological and Analytical Aspects, *Deutsche Lebensmittel-Rundschau* (1995). [in Germany]

[3] Hasanbeigi A., Hasanabadi A., Abdorrazaghi M., Comparison Analysis of Energy Intensity for Five Major Sub-Sectors of the Textile Industry in Iran, *J. Cleaner Production*, **23**(1): 186-194 (2012).

[4] Solís M., Solís A., Pérez H.I., Manjarrez N., Flores M., Microbial Decolouration of Azo Dyes: A Review, *Process Biochemistry*, **47(**12): 1723-1748 (2012).

[5] Hajira T., Masooda Q., Uroos A., Roohina M.H., To Study the Effectiveness of Modified Surface of Lignocellulosic Material for the Removal of Reactive Red 223 by Adsorption Method, *Intern. Jou. of Curren. Res.*, **7**(3): 13888-13895 (2015).

[6] Nageswara Rao A., Lathsree, Sivasankar S., Sadasivam B.V., Rengaraj K., Removal of Azo Dyes from Aqueous Solutions Using Activated Carbon as an Adsorbent, *J. Env. Sci& Eng.*, **46**(2): 172-178 (2004).

[7] Namasivayam C., Kanchana N., Waste Banana Pith as an Adsorbent for Color Removal from Waste Water, *Chemosphere*, **25**(11): 1691-1705 (1992).

[8] Kannan N., Ramamoorthy K., Studies on the Removal of Dyes by Adsorption on Orange Peel., *Ind. J. Env. Prot*, **25**(5): 410-416 (2005).

[9] Saad M., Hajira T., Fakhra S., Synthesis and Characterization of SnO-CoO Nanocomposites by Bottom up Approach and Their Efficacy for the Treatment of Dyes Assisted Simulated Waste Water, *Intern. J. of Curr. Res.*, **7**(12): 23542-23550 (2015).

[10] Rahmat N.A., Ali A.A., Hussain N., Muhamad, M.S., Kristanti, R.A., Hadibarata, T., Removal of Remazol Brilliant Blue R Aqueous Solution by Adsorption Using Pineapple Leaf Powder and Lime Peel Powder, *Water, Air, & Soil Pollution*, **227**(4): 1-11 (2016).

[11] Faruk O., Bledzki A.K., Fink H.P., Sain, M., Progress Report on Natural Fiber Reinforced Composites, *Macromolecular Materials and Engineering*, **299**(1): 9-26 (2014).

[12] Srinivasan R.K., Advances in Application of Natural Clay and Its Composites in Removal of Biological, Organic, and Inorganic Contaminants from Drinking Water, *Advances in Materials Science and Engineering*,**2011**: 1- 17 (2011).

[13] Tahir H., Comparative Trace Metal Contents in Sediments and Liquid Wastes from Tanneries and the Removal of Chromium Using Zeolite-5A, *Electron. J. Environ. Agric. Food Chem.*, **4** (4): 1021-1032 (2005).

[14] Candiano G., Bruschi M., Musante L., Santucci L., Ghiggeri G.M., Carnemolla B., Orecchia P., ZardiL.,Righetti P. G., Blue Silver: A Very Sensitive Colloidal Coomassie G-250 Staining for Proteome Analysis, *Electrophoresis*, **25** (9): 1327–1333 (2004).

[15] Wainwright M., Phoenix D.A., Rice L., Burrow S.M., Waring J., Increased Cytotoxicity and Phototoxicity in the Methylene Blue Series via Chromophore Methylation, *Photochem. Photobiol. B*, **40**(3): 233-239 (1997).

[16] Aksua Z., Ertuğrulb, S. DönmezbG., Methylene Blue Biosorption by Rhizopus Arrhizus: Effect of SDS (Sodium Dodecyl Sulfate) Surfactant on Biosorption Properties, *Chem. Eng. Journal*,**158** (3): 474–481 (2010).

[17] Salager J.L., Surfactants Types and Uses. Fire p Booket-E300-Attaching Aid in Surfactant Science and Engineering in English. *Merida Venezuela*, **2**, (2002).

[18] Ash M., Ash I.,Handbook of Industrial Surfactants; Gower Pub.Company, *Aldershot, UK* (1993).

[19] Crini G., Non-Conventional Low-cost Adsorbents for Dye Removal: A Review, *Bioresource Technology*, **97**(9): 1061-1085 (2006).

[20] Jan M., David M., Rafael D., Ondrej S., Marketa P.,Martin D., Kamil K., Synthesis and Disinfection Effect of the Pyridine-4-aldoxime Based Salts., *Molecules*. **20**(3): 3681-3696 (2015).

[21] Aswal V.K., Deepshikha S., Goyal P.S., Bhattacharya S., Heenan R.K., Micellar Structures of Dimeric Surfactants with Phosphate Head Groups and Wettable Spacers: A Small-Angle Neutron Scattering Study. *In: Physical Review E - Statistical Physics, Plasmas, Fluids, and Related Interdisciplinary Topics*, **59** (3): 3116-3122 (1999).

[22] Hashimoto K., Miura K., Kyotani S., Regeneration of Activated Carbons Used in Waste-Water Treatment by a Moving-Bed Regenerator, *AIChE journal*, **31**(12): 1986-1996. (1985).

[23] Khobragade M.U., Pal A., Surfactant Adsorption on Solid Surfaces and Further Application to Adsolubilization: *A Comprehensive Review. Recent Patents on Engineering*, **7**(3): 167-181. (2013).

[24] Das A.K., Saha S., Pal A., Maji S.K., Surfactant-Modified Alumina: An Efficient Adsorbent for Malachite Green Removal from Water Environment, *J. Environ. Sci. and Health, Part A*, **44**(9): 896-905 (2009).

[25] Almeida C.A.P., Debacher N.A., Downs A.J., Cottet L., Mello C.A.D., Removal of Methylene Blue from Colored Effluents by Adsorption on Montmorillonite Clay, *J. Colloïd and Interface Science*, **332**(1): 46-53 (2009).

[26] Saitoh T., Saitoh M., Hattori C., Hiraide M., Rapid Removal of Cationic Dyes from Water by Coprecipitation with Aluminum Hydroxide and Sodium Dodecyl Sulfate, *J. Environ. Chem. Eng*., **2**(1): 752-758 (2014).

[27] Poon J., Batchelor-McAuley C., Tschulik K., Compton, R. G., Single Graphene Nanoplatelets: Capacitance, Potential of Zero Charge and Diffusion Coefficient, *Chemical Science*, **6**(5): 2869-2876. (2015).

[28] DąbrowskiA., Adsorption-from Theory to Practice, *Adv. in Colloid and Interface Science*, **93**(1-3): 135-224 (2001).

[29] El Ouardi M., Qourzal S., Alahiane S., Assabbane A. Douch J., Effective Removal of Nitrates Ions from Aqueous Solution Using New Clay as Potential Low-Cost Adsorbent, *J. Encapsulation and Adsorption Sciences*, **5**(04): 178-190 (2015).

[30] Albadarin A.B., Mo J., Glocheux Y., Allen S., Walker G., Mangwandi C.,Preliminary Investigation of Mixed Adsorbents for the Removal of Copper and Methylene Blue from Aqueous Solutions, *Chemical Engineering Journal*, **255**(1): 525-534, (2014).

[31] Itodo A.U., Itodo H.U., Sorbent Capacities and Intensities of Thermo-Chemically Cracked Shea Nut Shells for the Removal of Waste Water Dyestuff, *Academia Arena*, **2**(3): 41-50. (2010).

[32] Mdoe J.E.G., Mkayula L.L., Adsorption of Gold on Activated Carbons Prepared from Some Tanzanian Carbonaceous Agrowastes and Bituminous Coal, *Bulletin of the Chemical Society of Ethiopia*, **10**(1): 21-32 (1996),

[33] Chuan-Wei Oo., Hasnah O., Sharon F., MaizatulAkmar Md. Z., The Uptake of Copper (II) Ions by Chelating Schiff Base Derived from 4-Aminoantipyrine and 2-Methoxybenzaldehyde, *Intern. J. of Nonferrous Metallurgy*, **2**: 1-9 (2013).

[34] Hong J. He S., Zhang L.A., Gan F.X., Ho Y.S., Equilibrium and Thermodynamic Parameters of Adsorption of Methylene Blue onto Rectorite, *Fresen. Env. Bulletin.*, **19**(11a): 2651-2656 (2010).

[35] Ghasemi M., Ghoreyshi A.A., Younesi H., Khoshhal S., Synthesis of a High Characteristics Activated Carbon from Walnut Shell for the Removal of Cr (VI) and Fe (II) from Aqueous Solution: Single and Binary Solutes Adsorption, *Iranian J. of Chem. Eng.*, **12**(4): 29 (2015).

[36] Suteu D., Malutan T., Industrial Cellolignin Wastes as Adsorbent for Removal of Methylene Blue Dye from Aqueous Solutions, *Bio Resources*, **8**(1): 427-446 (2012).

[37] Aksu Z., Application of Biosorption for the Removal of Organic Pollutants: A Review, *Process Biochemistry*, **40**(3): 997-1026 (2005).

[38] Naseem R., Tahir S.S., Removal of a Cationic Dye from Aqueous Solutions by Adsorption Onto Bentonite Clay, *Chemosphere*, **63** (11): 1842-1848 (2006).

[39] Manceau A., The Mechanism of Anion Adsorption on Iron Oxides: Evidence for the Bonding of Arsenate Tetrahedra on Free Fe $(O, OH)_6$ Edges, *Geochimica et Cosmochimica Acta*, **59**(17): 3647-3653. (1995).

[40] Thakur V.K., Thakur M.K., Gupta R.K., Graft Copolymers of Natural Fibers for Green Composites, *Carbohydrate Polymers*, **104**: 87-93. (2014).

[41] Huang S.H., Chen D.H., Rapid Removal of Heavy Metal Cations And Anions from Aqueous Solutions by an Amino-Functionalized Magnetic Nano-Adsorbent, *J. Hazardous Materials*, **163**(1): 174-179 (2009).